

Suppression of the anti-symmetry channel in the conductance of telescoped double-wall nanotubes

Ryo Tamura

Faculty of Engineering, Shizuoka University, 3-5-1 Johoku, Hamamatsu 432-8561, Japan

Yoko Sawai and Junji Haruyama

Aoyama Gakuin University, 5-10-1 Huchinobe, Sagamihara, Kanagawa 229-8558, Japan

Abstract

The conductance of telescoped double-wall nanotubes (TDWNTs) composed of two armchair nanotubes $((n_O, n_O)$ and $(n_O - 5, n_O - 5)$ with $n_O \geq 10$) is calculated using the Landauer formula and a tight binding model. The results are in good agreement with the conductance calculated analytical by replacing each single-wall nanotube with a ladder, as expressed by $(2e^2/h)(T_+ + T_-)$, where T_+ and T_- are the transmission rates of the symmetry and anti-symmetry channels, respectively. Perfect transmission in both channels is possible in this TDWNT when $n_O = 10$, while T_- is considerably small in the other TDWNTs. T_- is particularly low when either n_O or $n_O - 5$ is a multiple of three. In this case, a three body effect of covalent-like interlayer bonds plays a crucial role in determining the finite T_- . When n_O is a multiple of five, the five-fold symmetry increases T_- , although this effect diminishes with increasing n_O .

I. INTRODUCTION

The miniaturization of electronic devices will reach real physical limits in the near future, such as the breakdown of ultra-thin leads at high current densities. Carbon nanotubes (NTs), with the ability to carry much higher current densities than metal, are therefore expected to become an important component in future devices. This improved current capacity derives from the strong covalent bonds that make up the honeycomb lattice of the NTs. Metallic and semiconducting NTs have also been developed, representing potentially important elements of electronic circuitry [1]. While the general applicability of single-walled nanotubes (SWNTs) in electronic circuits is feasible, the problem of assembling SWNTs into complex systems remains to be overcome. For example, seamless junctions with disclinations [2,3], as well as cross junctions [4], and Y-shaped nanotubes [5] are necessary circuit features.

Recently, new types of NT junctions have been prepared from multi-wall nanotubes (MWNTs) by electrical breakdown of successive layers [6] and by “telescoping” the MWNT [7,8]. In such telescoped MWNTs (TMWNT), the inner core NT is attached to a scanning probe tip and pulled out from the outer NT. In these systems, the SWNT is assembled by interlayer interaction. Thus, the nature of the interlayer interaction is important in terms of both the electronic characteristics and the mechanical properties of the resultant SWNT network [9].

As a special type of MWNT, double-wall nanotubes (DWNTs) are prepared from a C₆₀-filled SWNT [10] or by catalytic chemical vapor deposition of acetylene with zeolite [11]. Energy bands [12] and the conductance [13] of DWNTs have been theoretically investigated. This paper discusses the electronic characteristics of telescoped double-wall nanotubes (TD-WNTs), as illustrated in Fig. 1, as the most simple example of a TMWNT. In a TDWNT, the path of the current along each SWNT is broken between the source electrode and the drain electrode to force the net current to flow between the layers. Thus, the effect of the interlayer connection is much stronger than in un-telescoped DWNTs. This enhanced effect is suitable for controlling the current by modifying the interlayer configuration. Further-

more, the interlayer configuration can be controlled directly with angstrom accuracy by adjusting the exact position on the scanning probe to which the TDWNT is attached, as the honeycomb lattice of the TDWNT is resistant to deformation as long as the inner and outer SWNTs are maintained parallel. This stability originates from the stronger intra-layer σ bond compared to the interlayer connection, making repeatable control of the electronic current possible.

Although the conductance of TDWNTs has been calculated using the Landauer formula [14–16], there remains some controversy regarding the result. For example, the maximum conductance of a TDWNT composed of a (10, 10) armchair NT and a (5, 5) NT is less than G_0 in Ref. [14], but close to $2G_0$ in Ref. [15], where G_0 represents the quantum conductance $2e^2/h$. In other word, the two conduction channels are open in the former, while one is closed in the latter. As mentioned above, change of the interlayer configuration can modify the conductance significantly even when the change is smaller than an angstrom, but it was not discussed in these References [14,15]. Thus we suppose that the disagreement arises from small difference in the interlayer configuration. In order to confirm this supposition, the conductance of TDWNT composed of two armchair nanotubes is calculated using two models, a tube model and a ladder model. The tube model directly represents the structure of the TDWNT and gives a numerical result, whereas ladder model gives analytical results, providing a physical picture not found in other theoretical papers [14–16]. In the analytical conductance of Ref. [14], the procedure for obtaining numerical values of the parameters k_1, k_2 and ϵ was not shown. Thus, it is only possible to reproduce their numerical results by fitting their analytical expression. In contrast, all the parameters in the present analytical conductance are determined discretely, and the results are in good agreement with the numerical outcome using the tube model. This makes it possible to clarify whether the two conduction channels are indeed open or not.

II. METHODOLOGY

The outer and inner tubes are denoted by ' O ' and ' I '. To simplify the discussion, both tubes are defined as armchair tubes, (n_O, n_O) and (n_I, n_I) . As the interlayer distance must be close to that of graphite, only the case of $n_O = n_I + 5$ is considered here. The common tube axis is defined as the z axis in cylindrical coordinates (r, θ, z) . An atom in tube μ ($\mu = O, I$) is expressed as (μ, l, i) , where integers l and i increase with z and θ , respectively. For the $(2, 2)$ armchair tube, the correspondence between (θ, z) and (l, i) is shown in Fig. 2. Tight binding (TB) models and Landauer formula are used to calculate the conductance in both the tube and ladder models, as shown below.

A. Tube model

The amplitude of the wave function at (μ, l, i) is defined as $\psi_{l,i}^{(\mu)}$. In Fig. 3, $\vec{\psi}_l^{(\mu)}$ represents the wave function in a half unit cell, as given by ${}^t\vec{\psi}_l^{(\mu)} = (\psi_{l,1}^{(\mu)}, \psi_{l,2}^{(\mu)}, \dots, \psi_{l,2n_\mu}^{(\mu)})$. With the lattice constant a ($\simeq 0.25$ nm) and a fractional shift Δz ($|\Delta z| < 0.5a$), sites (I, l, i) and (O, l, i) are located at $z = (l + 1)0.5a$ and $z = \Delta z + (l + 1)0.5a$, respectively. The relative rotation of the two SWNTs is represented by $\Delta\theta \equiv \theta_{0,1}^{(I)} - \theta_{0,1}^{(O)}$, where $\theta_{l,i}^{(\mu)}$ denotes θ at (μ, l, i) . The maximum l for $\vec{\psi}_l^{(I)}$ is equal to $2L - 2$, where L represents the number of unit cells in the DWNT region, that is, $L = 2$ in Fig. 3. For $-1 \leq l \leq 2L - 2$, that is, when l is in the DWNT region, ' D ' is used to express ${}^t\vec{\psi}_l^{(D)} \equiv ({}^t\vec{\psi}_l^{(I)}, {}^t\vec{\psi}_l^{(O)})$. The wave function in a full unit cell is given by \vec{e}_N as follows.

$${}^t\vec{e}_N = ({}^t\vec{\psi}_{2N-1}^{(\mu)}, {}^t\vec{\psi}_{2N}^{(\mu)}) , \quad (1)$$

where $\mu = I$ is the I SWNT region ($N \leq -1$), $\mu = D$ is the central DWNT region ($0 \leq N \leq L - 1$), and $\mu = O$ is the O SWNT region ($L \leq N$).

The present analysis employs the same TB model with π orbitals as used to investigate multilayer graphite and DWNTs in Ref. [17]. The intra-layer Hamiltonian matrix elements

between nearest neighbors are constant values of $-t = -2.75$ eV, and other intra-layer elements are zero. The TB equation for the energy E is expressed as

$$-P_2^{(\mu)} \vec{\psi}_{2N+1}^{(\mu)} = {}^t P_1^{(\mu)} \vec{\psi}_{2N-1}^{(\mu)} + (G_2^{(\mu)} - E) \vec{\psi}_{2N}^{(\mu)} \quad (2)$$

and

$$(G_1^{(\mu)} - E) \vec{\psi}_{2N+1}^{(\mu)} + P_1^{(\mu)} \vec{\psi}_{2N+2}^{(\mu)} = -{}^t P_2^{(\mu)} \vec{\psi}_{2N}^{(\mu)}, \quad (3)$$

under the condition that the Hamiltonian matrix element between (μ, l, i) and (μ, m, j) vanishes when $|l - m| > 1$. This condition is satisfied when $N \leq -2$ and $L \leq N$, that is, when N is in the SWNT region. In this case, the matrixes P_1 and P_2 become the scalar $-t$. Equations (2) and (3) can then be combined as a matrix equation,

$$A_\mu \vec{e}_{N+1} = B_\mu \vec{e}_N, \quad (4)$$

and the transfer matrix in each SWNT region can be obtained as $T_\mu = A_\mu^{-1} B_\mu$. Solving the eigenvalue problem, $T_\mu \vec{u}_i^{(\mu)} = \lambda_i^{(\mu)} \vec{u}_i^{(\mu)}$, the wave function \vec{e}_N in the μ SWNT region can be expressed as

$$\vec{e}_N = \sum_{i=1}^{2n_\mu} ((\lambda_i^{(\mu)})^N \vec{u}_i^{(\mu)} x_i^{(\mu)} + (\lambda_{i+2n_\mu}^{(\mu)})^N \vec{u}_{i+2n_\mu}^{(\mu)} y_i^{(\mu)}), \quad (5)$$

where $\vec{u}_i^{(\mu)}$ ($\vec{u}_{i+2n_\mu}^{(\mu)}$) refers to a propagating wave or an evanescent wave moving in the $+z$ direction ($-z$ direction).

The interlayer interaction is much weaker than the intra-layer bond and is sometimes classified as a van der Waals interaction. Nevertheless, the character of the interlayer interaction is similar to that of the covalent bond as it is caused by overlap between the π orbitals of neighboring layers. Therefore, the interlayer interaction can be represented by the hopping integral of the TB model to reflect its covalent character, that is, anisotropy and a finite number of bonds per atom. Reflecting these characteristics, the hopping integral between site i in the O tube and site j in the I tube is represented by

$$H_{i,j} = W_{i,j} \cos(\theta_i - \theta_j) \exp[-(d_{i,j} - \delta)/L_c], \quad (6)$$

where $\delta = 0.334$ nm, $L_c = 0.045$ nm, and $d_{i,j}$ is the distance between i and j [17]. The interlayer bonds are classified as AA bonds, BB bonds and AB bonds. For the AA and BB bonds, $W_{i,j} = 0.36$ eV, while $W_{i,j} = 0.16$ eV for the AB bond. The definition of these three types are as follows. For $d_{i,j}^2 < d_0^2 + r_0^2$, where d_0 equals the interlayer distance and $r_0 = 0.36a/\sqrt{3}$, an AA bond is formed between i and j . This condition guarantees that the number of AA bonds per atom is either zero or one. When an atom has an AA bond, the other interlayer bond of the atom is weakened due to saturation of the covalent bond number; when either site i or site j is connected with the third site k by an AA bond, the bond between site i and site j becomes an AB bond (Fig. 4 (c) and (d)). Otherwise, the connection is made by a AA or BB bond (Fig. 4 (a) and (b)). In Fig. 4, the atom of the outer tube forms an AA bond when it comes within the area designated by the dashed oval. It should be noted that $H_{i,j}$ in (c) and (d) is smaller than that in (b) for the same $d_{i,j}$ and $\theta_i - \theta_j$. Hereafter, this character of the interlayer hopping integral is referred to as the “three body effect”, in which $H_{i,j}$ is determined not only by atoms i and j but also by the third atom k . The importance of the three body effect will be discussed latter.

For $d_{i,j}^2 > D^2 + r_1^2$, $W_{i,j} = 0$, where r_1 is the “cutoff”. According to Ref. [17], r_1 is defined as $1.37a/\sqrt{3}$. As $\Delta z = 0$ in the usual stacking of graphite, only the case of small $|\Delta z|$ is considered here. Owing to the cutoff r_1 and small $|\Delta z|$, it is not necessary to consider the interlayer hopping integral between $\vec{\psi}_l^{(O)}$ and $\vec{\psi}_m^{(I)}$ when $|l - m|$ is larger than unity. In this case, eqs. (2), (3) and (4) can also be used for the DWNT region, where $0 \leq N \leq L - 2$ and $\mu = D$. This gives the transfer matrix in the DWNT region, $T_D = A_D^{-1}B_D$.

Equations similar to eq. (4) can then be obtained, $A_{ID}\vec{e}_0 = B_{ID}\vec{e}_{-1}$ and $A_{DO}\vec{e}_L = B_{DO}\vec{e}_{L-1}$, at the boundary between the SWNT and DWNT regions. However, the transfer matrix cannot be calculated in this case because A_{ID} and A_{DO} are not square matrices and do not have inverses. In this case, the conditioned transfer matrix can be calculated instead [3]. The pseudo-inverse matrix \tilde{X} is defined as $\tilde{X} \equiv (X^\dagger X)^{-1}X^\dagger$ for the matrix X with dimensions $p \times q$ and rank q ($p > q$). Since $\tilde{X}X = 1$ and $\vec{e}_{L-1} = T_D^{L-1}\vec{e}_0$,

$$\tilde{B}_{ID}A_{ID}\vec{e}_0 = \vec{e}_{-1} \quad (7)$$

and

$$\tilde{A}_{DO}B_{DO}T_D^{L-1}\vec{e}_0 = \vec{e}_L \quad . \quad (8)$$

However, the vectors \vec{e}_0 cannot be chosen arbitrary because $X\tilde{X} \neq 1$. The necessary conditions are then

$$(B_{ID}\tilde{B}_{ID}A_{ID} - A_{ID})\vec{e}_0 = 0 \quad (9)$$

and

$$(A_{DO}\tilde{A}_{DO}B_{DO} - B_{DO})T_D^{L-1}\vec{e}_0 = 0 \quad . \quad (10)$$

Using eq. (5) to represent \vec{e}_{-1} and \vec{e}_L , the wave function of the TDWNT can be expressed by $\vec{x}^{(I,O)}$, $\vec{y}^{(I,O)}$ and \vec{e}_0 . These vectors have $8(n_I + n_O)$ components and must satisfy the conditions (7), (8), (9) and eq.(10), where total number of independent conditions is $6n_I + 6n_O$; $4n_I$ in eq. (7), $4n_O$ in eq. (8), $2n_O$ in eq. (9), and $2n_I$ in eq. (10). Note that not all the rows of the matrix are independent in eqs. (9) and (10). Using the $4(n_I + n_O)$ conditions to eliminate \vec{e}_0 , the other $2(n_I + n_O)$ conditions can be represented by

$$\begin{pmatrix} \vec{y}^{(I)} \\ \vec{x}^{(O)} \end{pmatrix} = \begin{pmatrix} S_{I,I} & S_{I,O} \\ S_{O,I} & S_{O,O} \end{pmatrix} \begin{pmatrix} \vec{x}^{(I)} \\ \vec{y}^{(O)} \end{pmatrix} \quad (11)$$

with the scattering matrix S , which describes the outgoing waves (${}^t\vec{y}^{(I)}, {}^t\vec{x}^{(O)}$) as a function of the incoming waves (${}^t\vec{x}^{(I)}, {}^t\vec{y}^{(O)}$). The cases where E is close to the half-filled Fermi level, that is, $E \simeq 0$, are considered here such that the channel number is two for both the (n_O, n_O) and (n_I, n_I) NTs. Assigning the propagating waves to the terms with $i = 1, 2$ in eq. (5), the conductance is given by $G_0\Sigma_{i=1,2}\Sigma_{j=1,2}|(S_{I,O})_{i,j}|^2$ according to the Landauer formula with a quantum conductance of $G_0 = 2e^2/h$.

III. LADDER MODEL

In the ladder model, tubes I and O are replaced by ladders as shown in Fig. 5. The Hamiltonian of this model h is derived from H . Here, ϕ is used to represent the wave function in the ladder model to distinguish it from ψ in the tube model. When i and j have common parity, $\phi_{l,i}^{(\mu)}$ corresponds to $\psi_{l,j}^{(\mu)}$. The intra-layer elements of h are the same as those in H , with non-zero value $-t$ only between the nearest neighbors. The interlayer elements of h are defined based on the equation $E \sum_{\alpha} |\psi_{\alpha}|^2 = \sum_{\alpha, \beta} \psi_{\alpha}^* H(\alpha|\beta) \psi_{\beta}$, derived from the TB equation (l, i, μ in $\psi_{l,i}^{(\mu)}$ are abbreviated as α or β). In comparison with the similar equation of the ladder model with the normalization $|\vec{\psi}_l^{(\mu)}|^2 = |\vec{\phi}_l^{(\mu)}|^2$, we can show that

$$\sum_{\alpha, \beta} \phi_{\alpha}^* h(\alpha|\beta) \phi_{\beta} = \sum_{\alpha, \beta} \psi_{\alpha}^* H(\alpha|\beta) \psi_{\beta}. \quad (12)$$

In eq. (12), the interlayer terms on the right-hand side are assumed to coincide with those on the left as follows.

$$h(O, l, i|I, m, j) = \sum_{k'=1}^{n_I} \sum_{k=1}^{n_O} \frac{\psi_{l,2k+i}^{(O)*} H(\alpha|\beta) \psi_{m,2k'+j}^{(I)}}{\phi_{l,i}^{(O)*} \phi_{m,j}^{(I)}}, \quad (13)$$

where $\alpha = (O, l, 2k + i)$ and $\beta = (I, m, 2k' + j)$. Considering plane waves with the normalization $|\vec{\psi}_l^{(\mu)}|^2 = |\vec{\phi}_l^{(\mu)}|^2$, that is, $|\psi_{l,i}^{(\mu)} / \phi_{m,j}^{(\mu)}| = 1 / \sqrt{n_{\mu}}$,

$$h(O, l, i|I, m, j) = \frac{1}{\sqrt{n_I n_O}} \sum_{k'=1}^{n_I} \sum_{k=1}^{n_O} H'(\alpha|\beta). \quad (14)$$

Here, $\psi_{l,i}^{(\mu)} / \phi_{m,j}^{(\mu)}$ is replaced with $1 / \sqrt{n_{\mu}}$ in order to define h independently of ϕ and ψ .

Furthermore Hamiltonian of the tube model H is replaced by H' defined as

$$H'(O, l, i|I, m, j) = (1/2) \sum_{k=0}^1 H(O, l - m + k, i|I, k, j) \quad (15)$$

for the DWNT region, where $-1 \leq l \leq 2L - 1$, $-2 \leq m \leq 2L - 2$ and $l - m = 0, \pm 1$. When l and m are outside of this region, $H(O, l, i|I, m, j) = H'(O, l, i|I, m, j) = 0$. Because of the latter replacement, $h(O, l, i|I, m, j)$ with fixed i and j depends only on $l - m$ in the double ladder region.

By unitary transformation, $\tilde{\phi}_{l,\sigma}^{(\mu)} = (1/\sqrt{2})(\phi_{l,0}^{(\mu)} + \sigma\phi_{l,1}^{(\mu)})$ with $\sigma = \pm$, the ladder model can be considered to consist of four chains, (μ, σ) , with the following Hamiltonian matrix elements.

$$\begin{aligned}\tilde{h}(O, l, \sigma | I, m, \sigma') &= \frac{1}{2} \sum_{i=0}^1 \sum_{j=0}^1 \sigma^i (\sigma')^j h(O, l, i | I, m, j) \\ \tilde{h}(\mu, l, \sigma | \mu, m, \sigma) &= -\sigma t \delta_{l,m} - t(\delta_{l,m+1} + \delta_{l,m-1}) ,\end{aligned}\quad (16)$$

and $\tilde{h}(\mu, l, -\sigma | \mu, m, \sigma) = 0$. Owing to simplification represented by eq.(15), the hopping integral between the chains with common σ , that is $\tilde{h}(O, l, \sigma | I, m, \sigma)$, depends only on $l - m$ in the double chain region and denoted by $t_\sigma(l - m)$ as shown in Fig. 5(c). Although that between the chains with opposite σ , i.e., $\tilde{h}(O, l, -\sigma | I, m, \sigma)$, is not generally zero, it is neglected here in order to obtain the analytical transmission rate T_σ between the two chains with common σ , as given by

$$T_\sigma = \left| \frac{S_{0+}^2 \beta_+ + S_{0-}^2 \beta_- + C \beta_+^2 \beta_- + D \beta_+ \beta_-^2}{1 - S_{++}^2 \beta_+^2 - S_{--}^2 \beta_-^2 - 2 S_{+-}^2 \beta_+ \beta_- + \gamma \beta_+^2 \beta_-^2} \right|^2 \quad (17)$$

$$\beta_\tau = \exp(ik_\tau(2L - 1)) \quad (18)$$

$$C = -(S_{0+}S_{+-} - S_{0-}S_{++})^2 \quad (19)$$

$$D = -(S_{0+}S_{--} - S_{0-}S_{+-})^2 \quad (20)$$

$$\gamma = (S_{+-}^2 - S_{++}S_{--})^2 . \quad (21)$$

According to the Landauer formula, the conductance is $G_0(T_+ + T_-)$, where the quantum conductance is $G_0 = 2e^2/h$. Here, $S_{i,j}$ represents the scattering amplitude from channel j to channel i , where the propagating wave with wave number k_j corresponds to channel j ($j = 0, +, -$). Here, k_0 and k_\pm correspond to the plane wave in the single-chain region and the double-chain region, respectively (see Fig. 5(c)). These values are obtained as a function of the energy E and symmetry $\sigma = \pm$ by solving the following equations.

$$E = -\sigma t - 2t \cos k_0 \quad (22)$$

$$E = -\sigma t - 2t \cos k_\tau + \tau |f(k_\tau)| , \quad (23)$$

where $f(k_\tau)$ ($\tau = \pm$) is the effective inter-chain hopping defined by

$$f(k_\tau) = \sum_{j=-1}^1 t_\sigma(j) \exp(ik_\tau j) . \quad (24)$$

Although $S_{i,j}$ and k_j depend on σ , this relationship is not shown in eq. (17) explicitly in order to simplify the notation. The sign $\tau = +, -$ originates from the unitary transformation $(1/\sqrt{2})(\phi_{l,i}^{(I)} + \alpha_\tau \phi_{l,i}^{(O)})$, where

$$\alpha_\tau = \tau f(k_\tau)/|f(k_\tau)| . \quad (25)$$

Note that the sign τ is independent of the sign $\sigma = +, -$. The matrix S is symmetric and unitary, that is, $S^\dagger = S^{-1}$ and ${}^t S = S$, and is represented by the phase factors α_\pm and $w_j = \exp(ik_j)$ and by the group velocity $v_j = (1/t)(dE/dk_j)$ ($j = 0, +, -$) as follows.

$$S_{0,0} = -\frac{\text{Det}[w_0^*]}{\text{Det}} , \quad (26)$$

$$S_{\tau,\tau} = -\frac{\text{Det}[w_\tau^*, \alpha_\tau^*]}{\text{Det}} , \quad (27)$$

$$S_{0,\tau} = (-\tau i) \frac{\sqrt{2v_0 v_\tau \alpha_{-\tau}}}{w_{-\tau} \text{Det}} , \quad (28)$$

$$S_{+,-} = \sum_{s=\pm} s \left[\frac{\sqrt{v_-} \alpha_+^s (1 - w_0 w_+^{-s}) - t_\sigma(1) w_0 w_+^s}{\text{Det} \sqrt{v_+}} \right] \quad (29)$$

where

$$\text{Det} = \sum_{\tau=\pm} \tau \left[\frac{w_0 w_\tau + 1}{w_+ w_-} \sqrt{\frac{\alpha_{-\tau}}{\alpha_\tau}} - t_\sigma(1) \sqrt{\alpha_\tau} \right] \quad (30)$$

and $\text{Det}[w_0^*]$ in eq. (26) is defined by eq. (30) with w_0 replaced by its complex conjugate w_0^* . The symbols $\text{Det}[\dots]$ in eq. (27) have similar meaning.

IV. RESULTS AND DISCUSSION

Figure 6 shows the conductance of the (n_O, n_I) $i-j$ TDWNT for $E = 0.1$ eV as a function of the number of unit cells of the DWNT (L). Here, (n_O, n_I) $i-j$ denotes the TDWNT

composed of the (n_O, n_O) tube and (n_I, n_I) tube with rotation angle $\Delta\theta = i2\pi/(13n_O)$ and fractional overlap length $\Delta z = ja/(40)$, where the total overlap length is given by $La + \Delta z$. There is good agreement between the conductances of the ladder and tube models, verifying that eq. (17) can be used reliably to discuss the conductance.

Except for the $(10, 5)$ TDWNT, anti-symmetric channel transport is suppressed (the conductance does not reach $4e^2/h$) due to the effect of 'parity cancellation', that is, the terms in eq. (16) for the anti-symmetric channel ($\sigma = \sigma' = -1$) with even $i + j$ cancel with those with odd $i + j$ such that the interlayer hopping integral of the anti-symmetric channel t_- is always smaller than that of symmetric channel t_+ . This parity cancellation is weakened when $n_O (= n_I + 5)$ is a multiple of five. In order to show this effect, eq. (16) is rewritten as

$$t_-(l - m) = \sum_{k'=1}^{n_I} g(l - m, k') , \quad (31)$$

$$g(l - m, k') \equiv \frac{1}{\sqrt{n_I n_O}} \sum_{k=1}^{n_O} \sum_{i=0}^1 \sum_{j=0}^1 (-1)^{i+j} H'(\alpha|\beta) , \quad (32)$$

where $\alpha = (O, l, 2k + i)$ and $\beta = (I, m, 2k' + j)$. When the sign of $g(l - m, k')$ is changed randomly as a function of k' , t_- decreases as a result of parity cancellation. When n_I is a multiple of five, however, $g(l - m, k')$ is not random but a periodic function of k' , as follow.

$$t_-(l - m) = 5 \sum_{k'=1}^{n_I/5} g(l - m, k') \quad (33)$$

It is therefore apparent that the parity cancellation is weakened in eq. (33) compared to the case without five-fold symmetry. This effect is particularly enhanced when $n_I = 5$, and it is only under this condition that the conductance can reach $4e^2/h$ (Fig. 6). When $t_-(0) \simeq -t_-(1) \simeq -t_-(-1)$, however, the transmission rate of the anti-symmetric channel T_- is almost zero, even when $n_I = 5$ (see the $(10, 5)$ 0-0 TDWNT in Fig. 6(a)). This exceptional case is explained as follows. When $E = 0$ and $t_-(0) = -t_-(1) = -t_-(-1)$, the wave vector k_τ is equal to $\pi/3$, irrespective of τ . In that case, the effective hopping $f(k_\tau)$ defined by eq. (24) is zero, causing T_- to vanish.

The parity cancellation is enhanced when either n_O or n_I is a multiple of three. This enhanced parity cancellation is referred to as "three-fold cancellation". To simplify ex-

planation, the three body effect is neglected for a while. Without the three body effect, $H(O, l, i|I, m, j)$ in eq. (14) with fixed l and m depends only on $\theta_{l,i}^{(O)} - \theta_{m,j}^{(I)}$ and can be abbreviated to $H'(\theta_{l,i}^{(O)} - \theta_{m,j}^{(I)})$, where $\theta_{l,i}^{(O)}$ and $\theta_{m,j}^{(I)}$ represent θ of the (O, l, i) and (I, m, j) sites, respectively. Using the notation $\theta_{l,i \pm 2n_\mu}^{(\mu)} = \theta_{l,i}^{(\mu)}$ to represent the periodic boundary condition around the circumference, eq. (14) can be rewritten as

$$h(O, l, i|I, m, 0) = \frac{1}{\sqrt{n_I n_O}} \sum_{k'=1}^{n_I} \sum_{k=1}^{n_O} H'(\theta_{l,2k+i}^{(O)} - \theta_{m,2k'}^{(I)}) \quad (34)$$

and

$$h(O, l, i|I, m, 1) = \frac{1}{\sqrt{n_I n_O}} \sum_{\tilde{k}'=1}^{n_I} \sum_{\tilde{k}=1}^{n_O} H'(\theta_{l,2\tilde{k}+i}^{(O)} - \theta_{m,2\tilde{k}'+1}^{(I)}) . \quad (35)$$

In the following, we focus on the case of $n_O = n_I + 5$ being a multiple of three. Explanation for another case where $n_I = n_O - 5$ is a multiple of three can be easily derived from it. From Fig. 2, it can be shown that $\theta_{m,2k'}^{(I)} - \theta_{m,2\tilde{k}'+1}^{(I)}$ equals $(2\pi/3n_I)(3k' - 3\tilde{k}' - 2)$ for odd m and $(2\pi/3n_I)(3k' - 3\tilde{k}' - 1)$ for even m . Thus, $\theta_{m,2k'}^{(I)} - \theta_{m,2\tilde{k}'+1}^{(I)} = \pm 2\pi/3$ when $2k' - (2\tilde{k}' + 1) = \pm(2n_I + 1)/3$. Here, the upper and lower signs correspond to odd m and even m , respectively. On the other hand, $\theta_{l,2k+i}^{(O)} - \theta_{l,2\tilde{k}+i}^{(O)} = \pm 2\pi/3$ when $2k - 2\tilde{k} = \pm 2n_O/3$. Relating k and k' to \tilde{k} and \tilde{k}' in this way, it can be shown that $\theta_{l,2k+i}^{(O)} - \theta_{m,2k'}^{(I)} = \theta_{l,2\tilde{k}+i}^{(O)} - \theta_{m,2\tilde{k}'+1}^{(I)}$ in eqs. (34) and (35), that is, $h(O, l, i|I, m, 0)$ and $h(O, l, i|I, m, 1)$ have the same value and cancel out in $t_-(l - m)$ as defined by eq. (16). This means that the transmission rate of the $-$ channel is completely suppressed for arbitrary interlayer configurations $(\Delta\theta, \Delta z)$ under the condition that there is no three body effect. In order to illustrate this three-fold cancellation for the case where $n_O = n_I + 5 = 15, l = 0, m = 1$ and $i = 1$, Fig. 7 shows the corresponding honeycomb lattice with vertical axis θ and horizontal axis z for (a) $0 \leq \theta \leq 2\pi/3$, (b) $2\pi/3 \leq \theta \leq 4\pi/3$ and (c) $4\pi/3 \leq \theta \leq 2\pi$. In this case, the hopping integral between $(O, 0, 2k + 1)$ and $(I, 1, 2k')$ cancels that between $(O, 0, 2k - 9)$ and $(I, 1, 2k' - 7)$ in $t_-(-1)$. In Fig. 7, the interlayer bonds corresponding to the former and the latter are shown by the black and red lines, respectively, for the case of $k = 3p - 1$ and $k' = 2p$ with integers $p = 1, 2, \dots, 5$. These lines are labeled with the corresponding indexes of θ , i.e.,

$6p - 1, 4p, 6p - 11$ and $4p - 7$. In Fig. 7, the three-fold cancellation occurs between the interlayer bonds aligned at the same vertical position.

Taking the three body effect into account, however, the red bonds (BB) in Fig. 7 will have a larger hopping integral than the black bonds (AB). Here, the classification of the bond is determined by the dashed ovals; when an atom from each of tube I and tube O comes within the dashed oval, an AA bond is formed between them. This effect is illustrated in Fig. 8, where the three body effect has been removed by setting W_{ij} in eq. (6) to 0.36 eV irrespective of the type of bond (AA, AB and BB). The energy is the same as that in Fig. 6, that is, $E = 0.1$ eV. For comparison, the corresponding data in Fig. 6 are also shown in this figure. The maximum conductance of the $(15, 10)$ 4-1 TDWNT without the three body effect (dashed line) is close to G_0 , whereas that with the three body effect (triangles) reaches $1.2G_0$. The transmission rate of the anti-symmetric channel T_- is suppressed almost completely in the former case, whereas this suppression is relaxed in the latter. In this way, the three body effect increases the maximum conductance although it reduces the interlayer hopping integral of AB bonds. In contrast, the conductance exceeds G_0 considerably, irrespective of the three body effect, when neither n_O nor n_I is a multiple of three, as is indicated by the data for the $(10, 5)$ (-2) -0 TDWNT in Fig. 8.

The conductance tends to be larger when the TDWNT has five-fold symmetry without three-fold cancellation. This effect becomes smaller as n_I increases, as the terms $g(l - m, k')$ in eq. (33) may be positive or negative according to k' and therefore cancel. For example, compare the $(10, 5)$ TDWNT with the $(25, 20)$ TDWNT, both of which have five-fold symmetry but not three-fold cancellation. Among the 65 interlayer configurations $(\Delta\theta, \Delta z) = (i2\pi/(13n_O), ja/40)$, where $i = 0, 1, \dots, 12$ and $j = -2, -1, \dots, 2, 31$ configurations have conductance larger than $1.8G_0$ for the $(10, 5)$ TDWNT, whereas only 2 exceed this level for the $(25, 20)$ TDWNT. The conductance for this comparison was calculated by the tube model for $L \leq 100$.

The rapid oscillation and slow variation in the beat structures seen in Fig. 6 originate from the components with large wave numbers $2k_+, 2k_-, |k_+| + |k_-|$ in eq. (17) and from

those with small wave number $|k_+| - |k_-|$, respectively. As the weak interlayer hopping integral modifies the dispersion relation of the NT only slightly, the shift of $|k_{\pm}|$ from either $2\pi/3$ or $\pi/3$ is small. Therefore, the period of rapid oscillation is close to three and not much influenced by (n_O, n_I) , $\Delta\theta$ or Δz . In contrast, the period of the slow variation varies considerably with these parameters, as even small change in k_+ and k_- result in large relative changes in $|k_+| - |k_-|$. For example, the phase of the slow oscillation is almost reversed by a slight change in $\Delta\theta$ and Δz for $40 < L < 80$ (see Fig. 6(c)). In such cases, the lattice vibration modulating $\Delta\theta$ and Δz might obscure the beat structure, representing a possible reason for the lack of an apparent beat structure in previous experiments [8]. This sensitivity of the slow variation to $\Delta\theta$ and Δz is enhanced by the three body effect, where the change from a BB bond to an AB bond can be induced by a small change in $\Delta\theta$ or Δz .

Here, it should be noted that the first and second layers of the MWNT can be considered as TDWNTs in series when the outermost layer is broken down locally. If these two layers are armchair NTs and the current is concentrated in the outermost NT, the anti-symmetry channel of the MWNT is suppressed for the same reason as for the TDWNT. This may be one explanation for the single-channel transmission of MWNTs dipped in liquid metal [18]. Compared to the explanation considering interlayer interaction given in Ref. [19], the present explanation is relevant for a wider range of Fermi levels.

It is a unique character of TDWNTs that the three body effect has such a significant influence on the conductance. As the atomic motion changing an AB bond to a BB bond cannot be approximated by simple harmonic motion, it can be expected that interlayer vibration will give rise to new transport phenomena that differ from the usual phonon-assisted tunneling. Although the effect of interlayer vibration on the conductance in this case is an attractive subject, it will require massive numerical computation. A potential future direction for this work is therefore to extend the ladder model to overcome this difficulty. Intercalated TDWNTs are also attractive, as such a configuration should allow for the detection of current flowing through a small number of molecules or atoms between the layers without the need for an ultra-high vacuum or low temperatures. A simplified

Hamiltonian such as that of the ladder model will also be a powerful tool for this type of analysis.

In conclusion, conductances were calculated for telescoped double-wall nanotubes composed of two armchair nanotubes given by (n_O, n_O) and $(n_O - 5, n_O - 5)$ with $n_O \geq 10$. The interlayer displacement was found to alter the conductance significantly even when the movement is much smaller than the lattice constant. The conductance reaches the maximum value of the two channel system, $4e^2/h$, only when $n_O = 10$. In other TDWNTs, transport in the anti-symmetry channel is suppressed by parity cancellation. This parity cancellation is enhanced when either n_O or $n_O - 5$ is a multiple of three. In this case, the three body effect of the interlayer connection plays a crucial role in determining the finite transmission rate of the anti-symmetry channel. When n_O is a multiple of five, the five-fold symmetry reduces the parity cancellation, resulting in an increase in conductance. This effect of five-fold symmetry, however, diminishes with increasing n_O .

FIGURES

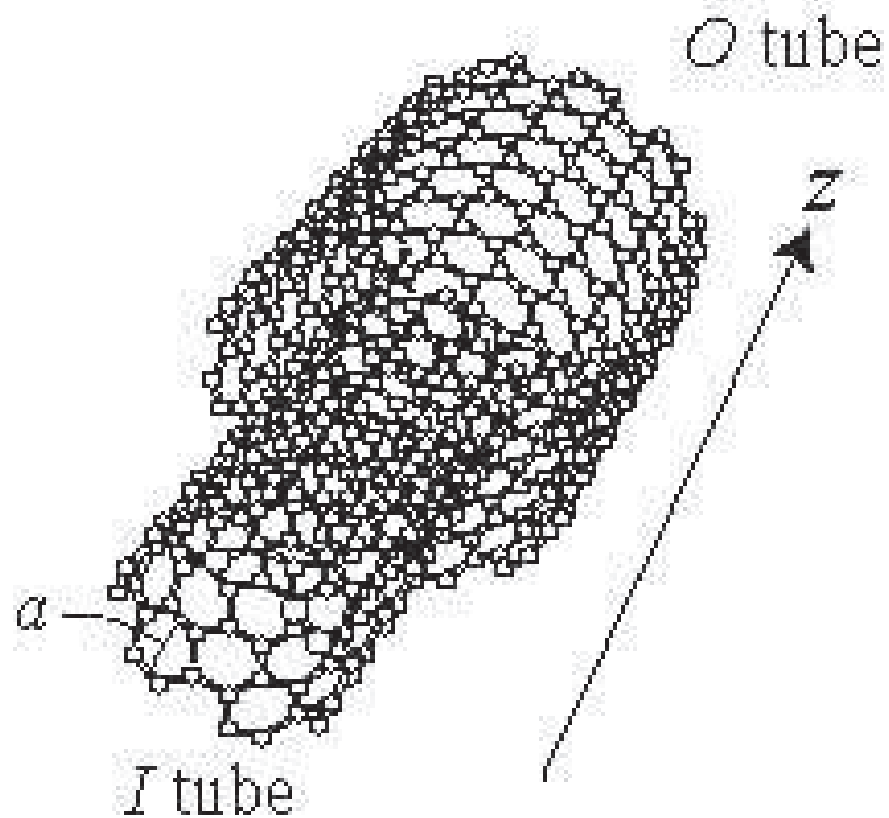


FIG. 1. Telescoped double-wall nanotube

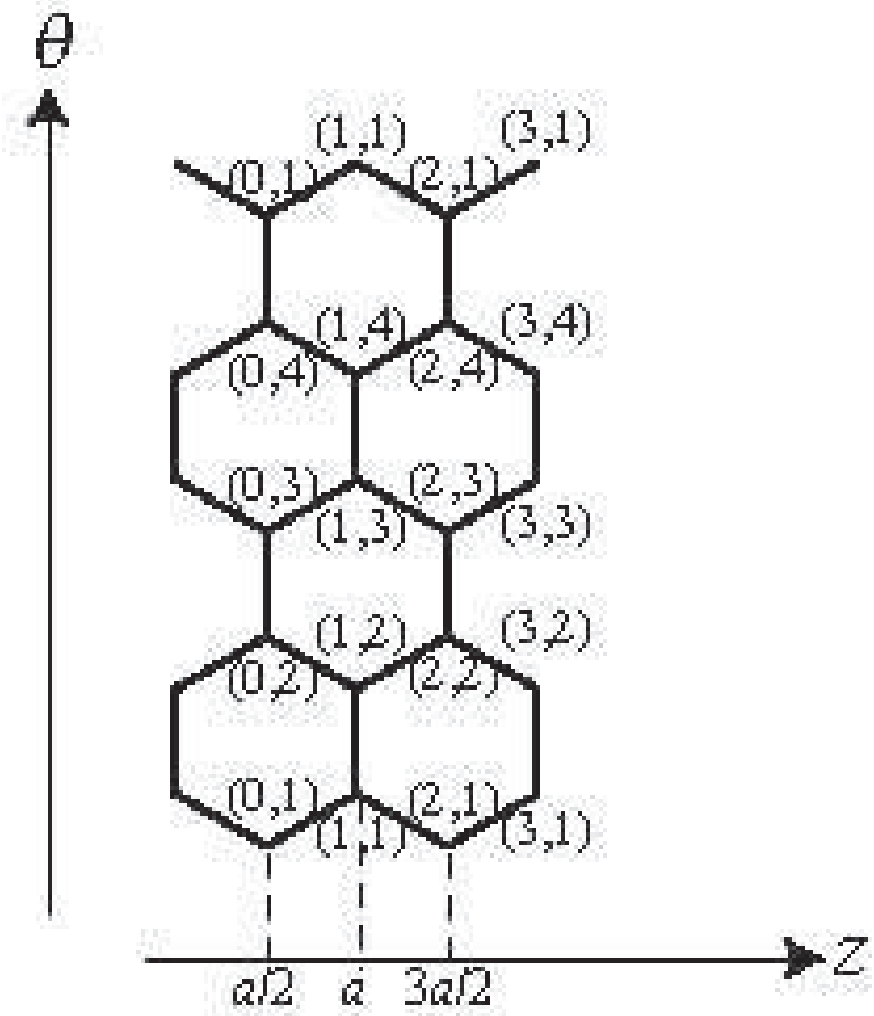


FIG. 2. Index (l, i) representing z and θ in a $(2, 2)$ armchair nanotube

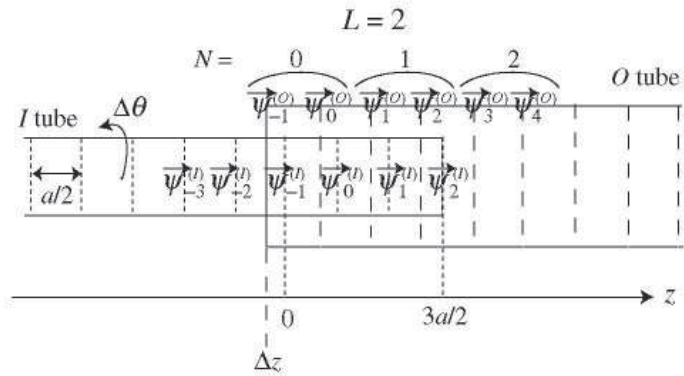


FIG. 3. Schema of a telescoped nanotube and amplitude of the wave functions $\vec{\psi}_l^{(O)}$ and $\vec{\psi}_l^{(I)}$ ($\Delta z < 0$)

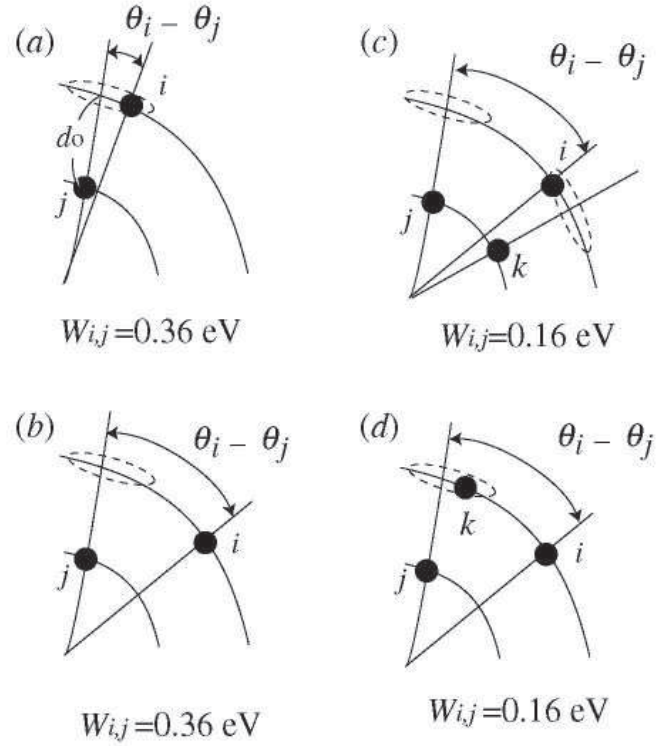


FIG. 4. Three body effect of the interlayer hopping integral. When the distance between i in tube O and j in tube I is smaller than $d_0^2 + r_0^2$, they are connected by an AA bond. This threshold is represented by dashed ovals. The other interlayer bonds of an atom with an AA bond are weakened due to saturation of the number of covalent bonds per atom. The hopping integral between i and j in (c) and (d) is smaller than that in (b) for the same sites i and j .

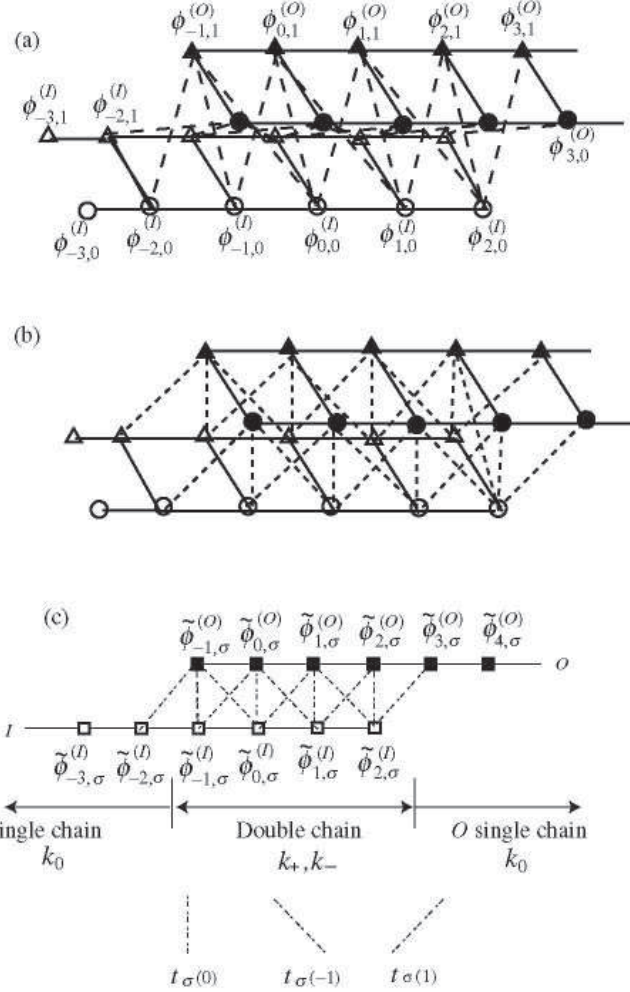


FIG. 5. Schema of ladder model and amplitude of the wave functions $\tilde{\phi}_l^{(O)}$ and $\tilde{\phi}_l^{(I)}$. The hopping integrals between the two ladders $h(O, l, i|I, m, j)$ are indicated by dashed lines in (a) and dotted lines in (b) for $i \neq j$ and $i = j$, respectively. (c) Ladder model after unitary transformation $\tilde{\phi}_{l,\sigma}^{(\mu)} = (1/\sqrt{2})(\phi_{l,0}^{(\mu)} + \sigma\phi_{l,1}^{(\mu)})$, where $\sigma = +, -$ and $\mu = O, I$.

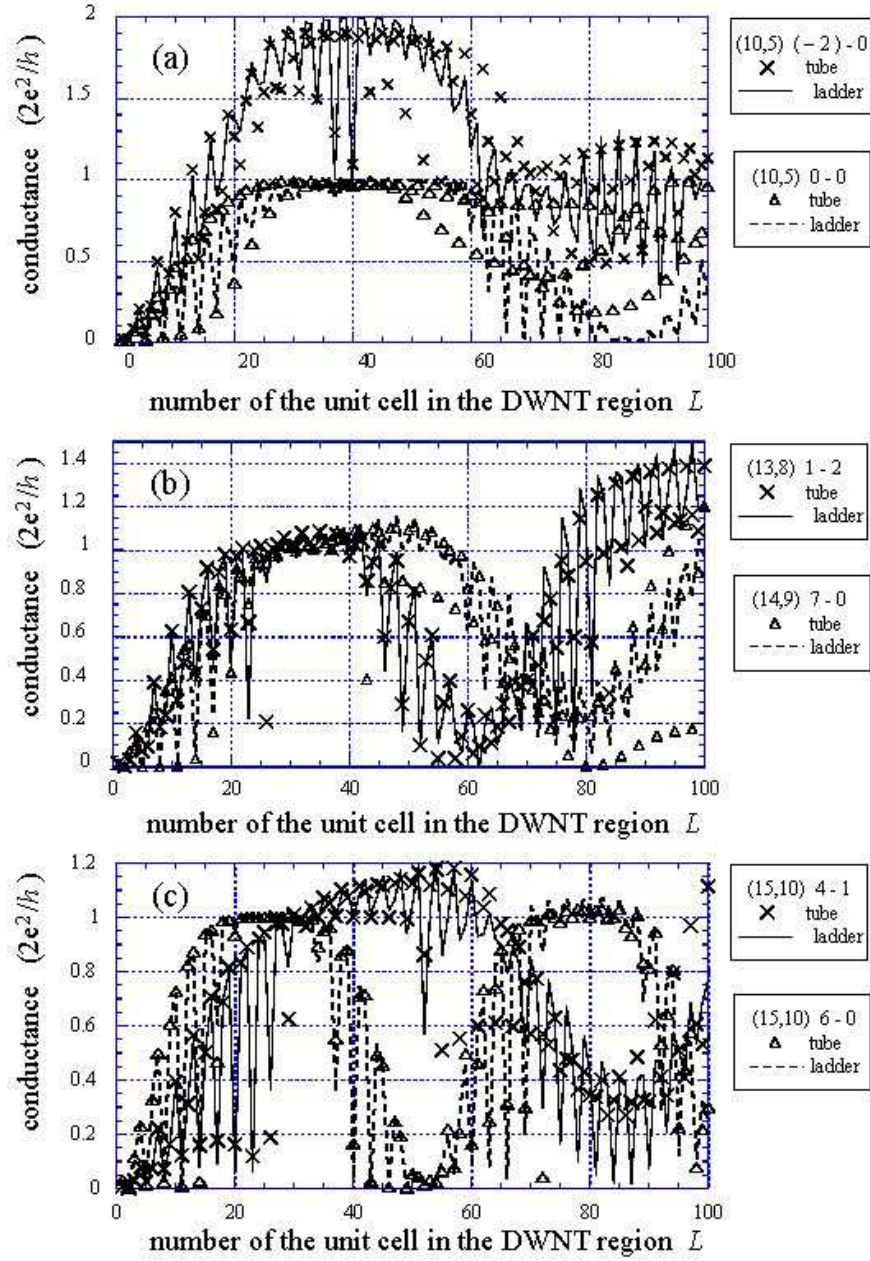


FIG. 6. Conductance of the (n_O, n_I) $i-j$ TDWNT at $E = 0.1$ eV

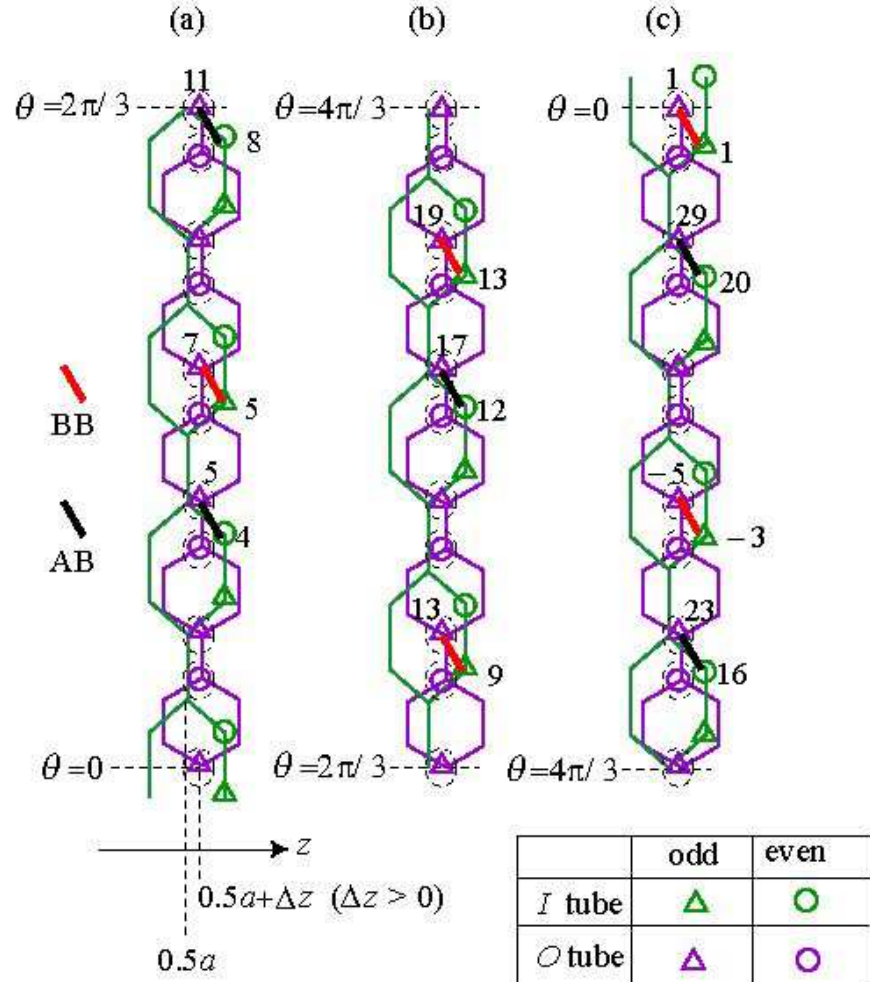


FIG. 7. Honeycomb lattice of the (15, 10) TDWNT near $z = 0$, with θ as the vertical axis and z as the horizontal axis, for (a) $0 \leq \theta \leq 2\pi/3$, (b) $2\pi/3 \leq \theta \leq 4\pi/3$ and (c) $4\pi/3 \leq \theta \leq 2\pi$. Black lines represents interlayer bonds between $(O, 0, 6p - 1)$ and $(I, 1, 4p)$, and red lines represent those between $(O, 0, 6p - 11)$ and $(I, 1, 4p - 7)$, with integers $p = 1, 2, \dots, 5$. These bonds are labeled with corresponding indexes of θ , i.e., $6p - 1, 4p, 6p - 11$ and $4p - 7$. Red and black lines with identical vertical position cancel out in the inter-chain hopping integral of the anti-symmetry channel. Red and black bonds represent BB and AB bonds, respectively.

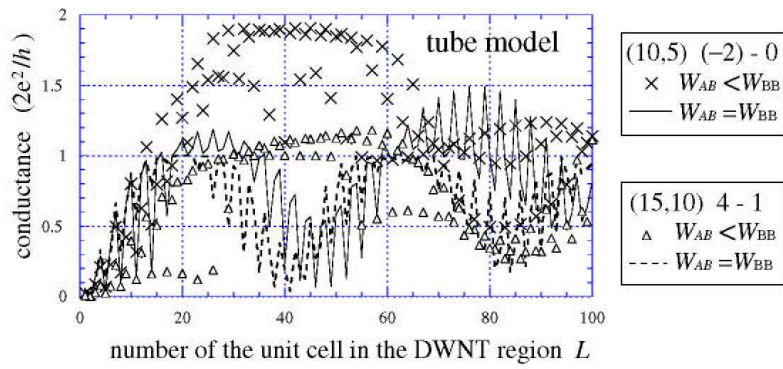


FIG. 8. Conductance of the tube model for $E = 0.1$ eV without the three body effect ($W_{AB} = W_{BB}$). Corresponding data from Fig. 6 shown for comparison ($W_{AB} < W_{BB}$).

REFERENCES

[1] N. Hamada, S. Sawada, and A. Oshiyama, Phys. Rev. Lett. **68**, 1579 (1992); J. W. Mintmire, B. I. Dunlap, and C. T. White, *ibid* **68**, 631 (1992); R. Saito, M. Fujita, G. Dresselhaus, and M. S. Dresselhaus, Phys. Rev. B **46**, 1804 (1992).

[2] Z. Yao, H. W. CH. Postma, L. Balents, and C. Dekker, Nature **402**, 273 (1999); R. Tamura, Phys. Rev. B. **67**, 121408 (2003); *ibid.* **64**, 201404 (2001); H. Matsumura and T. Ando, J. Phys. Soc. Jpn. **67**, 3542 (1998). ;L. Chico, Vincent H. Crespi, Lorin X. Benedict, Steven G. Louie, and Marvin L. Cohen, Phys. Rev. Lett. **76**, 971 (1996).

[3] R. Tamura and M. Tsukada, Phys. Rev. B. **61**, 8548 (2000).

[4] Y. -G. Yoon, M. S. C. Mazzoni, H. J. Choi, J. Ihm and S. G. Louie, Phys. Rev. Lett. **86** 688 (2001); M. Fuhrer, J. Nygard, L. Shih, M. Foreo, Y. -G. Yoon, M. S. C. Mazzoni, H. J. Choi, J. Ihm, S. G. Louie, A. Zettl, and P. L. McEuen, Science 288, 494 (2000).

[5] A. N. Andriotis, M. Menon, D. Srivastava and L. Chernozatonskii, Phys. Rev. B. **65** 165416 (2002); M. Menon and D. Srivastava, Phys. Rev. Lett. 79, 4453 (1997).

[6] J. Cumingsm P. G. Collins and A. Zettl, Science **289** 602 (2000). ; P. G. Collins, M. Hersam, M. Arnold, R. Martel, Ph. Avouris, Phys. Rev. Lett. **86**, 3128 (2001).

[7] J. Cumings and A. Zettl, Science **289** 602 (2000); Phys. Rev. Lett. **93** 086801 (2004).

[8] S. Akita and Y. Nakayama, J. J. Appl. Phys. **43** 3796 (2004).

[9] R. Saito, M. Matsumoto, T. Kimura, G. Dresselhaus and M. S. Dresselhaus, Chem. Phys. Lett. **348** 187 (2001); Y. K. Kwon and D. Tomanek, Phys. Rev. B **58** 16001 (1998); W. Guo, Y. Guo, H. Gao, Q. Zheng and W. Zhong. Phys. Rev. Lett. **91** 125501 (2003); Q. Zheng, J. Z. Liu and Q. Jiang, Phys. Rev. B **65**, 245409 (2002).

[10] S. Bandow, M. Takizawa, K. Hirahara, M. Yudasaka and S. Iijima, Chem. Phys. Lett. **337** 48 (2001)

- [11] T. Hiraoka et. al. , Chem. Phys. Lett. **382** 679 (2003).
- [12] R. Saito, G. Dresselhaus, and M. S. Dresselhaus, J. Appl. Phys. **73**, **494** (1993); Y. -K. Kwon and D. Tománek, Phys. Rev. B **58**, R16001 (1998); Y. Miyamoto, S. Saito, and D. Tománek, *ibid* **65**, 041402 (2001).
- [13] S. Uryu, Phys. Rev. B **69**, 075402 (2004). D. -H. Kim, H. -S. Sim, and K. J. Chang, *ibid* **64**, 115409 (2001);
- [14] D. -H. Kim and K. J. Chang, Phys. Rev. B, **66** 155402 (2002).
- [15] C. Buia, A. Buldum and J. P. Lu, Phys. Rev. B, **67** 113409 (2003);
- [16] A. Hansson and S. Stafstrom, *ibid* **67**, 075406 (2003).
- [17] Ph. Lambin, V. Meunier and A. Rubio, Phys. Rev. B **62** 5129 (2000); J. -C. Charlier, J. -P. Michenaud and Ph. Lambin, *ibid* **46** 4540 (2992).
- [18] S. Frank, P. Poncharal, Z. L. Wang, and W. A. de Heer, Science **280**, 1744 (1998).
- [19] S. Sanvito, Y. K. Kwon, D. Tomanek and C. J. Lambert, Phys. Rev. Lett, **84** 1974 (2000).